

## SIMULATION OF GROUND-COUPLED HEAT PUMP SYSTEMS USING A SPECTRAL APPROACH

**Philippe Pasquier<sup>1</sup>, Denis Marcotte<sup>1</sup>, Michel Bernier<sup>2</sup> and Michaël Kummert<sup>2</sup>**

Polytechnique Montréal, Montréal, Canada

<sup>1</sup>Department of Civil, Geological and Mining Engineering

<sup>2</sup>Department of Mechanical Engineering

### ABSTRACT

This paper presents a method using a spectral approach to simulate a hybrid ground-coupled heat pump system. At each time step, the algorithm computes the ground load based on the building load, the coefficient of performance and the capacity of the heat pumps (which are a function of the fluid temperature), and the equivalent borehole thermal resistance. To capture the nonlinearity between the fluid temperature and the ground load, an iterative process is used. Results show that the proposed method is efficient in predicting the number of operating heat pumps required to ensure that the fluid temperature always remains between the heat pumps operational temperature limits and that the total energy provided to the building never exceeds the total capacity of the heat pumps. The approach used solves the entire simulation duration in a single step. In the present case, an hourly simulation over a ten-year period is completed in less than 10 seconds.

### INTRODUCTION

Several approaches are available to simulate hybrid ground-coupled heat pump (HyGCHP) systems (Pahud and Hellström, 1996; Nagano et al., 2006; Gentry et al., 2007). Most approaches either integrate a set of ordinary differential equations, or convolve in the time domain an aggregated load signal. To account for the interactions between the fluid temperature, the performance and capacity of the heat pump (HP) as well as the ground and building loads, the solution process requires iterations at each time step before proceeding to the next step, which can lead to large computing time.

The design of HyGCHP systems requires several multi-year simulation runs. This leads to undesirably large design times for designers (Cullin and Spittler, 2011), who will then prefer simpler sizing approaches which are not necessarily optimum.

To reduce computation time, Marcotte and Pasquier (2008) convolved the response function of a borehole heat exchanger (BHE) field and a thermal load signal in the spectral domain. Using a combined FFT-Spline approach, they reported computing times up to 9000 times faster than convolution in the time domain.

To account for the temperature limits and the

capacity of the installed HPs, Marcotte et al. (2009) later integrated a spectral approach in a sequential iterative process. In their 2009 paper, Marcotte et al. treated the problem constraints sequentially, namely time step by time step, and reported computing time of 2 minutes for the hourly simulation of a 45 BHEs field over a 10-year period. Since then, questions have been raised about the overall efficiency of spectral approaches to treat non-linear coupled processes such as simulation of HyGCHP systems. The objective of this paper is to present a general and efficient computational methodology relying on a spectral approach to simulate a HyGCHP system.

The proposed approach is illustrated by simulating the system depicted in Fig. 1. In this system, water-to-water HPs are connected to a series of boreholes on the source side and to the building on the load side. They either provide heating or cooling to the building water loop, which then serves a series of water-to-air heat pumps. In order to reduce the size of the BHE field, some heat pumps are deactivated at peak conditions. During these conditions, an auxiliary heating or cooling system is activated. It is

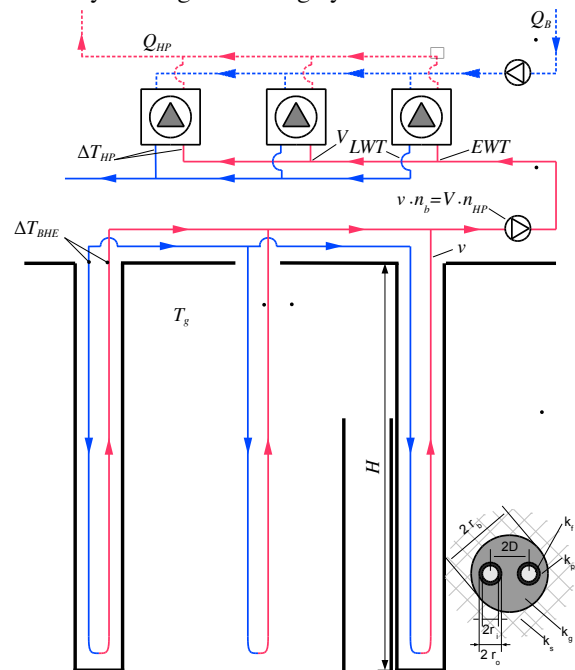


Figure 1: Layout of a hybrid ground-coupled heat pump system for a case where  $n_b = n = n_{HP} = 3$  in heating mode.

assumed here that these auxiliary systems will provide the necessary heating and cooling to cover the building load ( $Q_B$ ). A variable speed circulation pump is used on the source side. In this configuration, the HPs have the same entering water temperature and, if operating, have the same capacity. To maintain the fluid temperature within the HPs operational range, a control sequence decides whether HPs are on, off, or in cycling mode during a given time step. If more than one HP is operating, only one HP cycles at a given time to meet the load.

## METHODOLOGY

### Heat Transfer Model

For a constant ground thermal load  $q$  (W/m), the mean fluid temperature  $T_f$  (K) circulating in a BHE can be expressed by:

$$T_f(t) = T_g + q \cdot R_b + \frac{q}{2\pi k} g\left(\frac{t}{t_s}, \frac{r_b}{H}\right) \quad (1)$$

where  $T_g$  is the initial ground temperature (K);  $R_b$  is the equivalent borehole resistance (mK/W);  $k$  (W/(mK)) is the ground thermal conductivity;  $H$  is the borehole length (m),  $r_b$  is the borehole radius (m);  $t_s = H^2/9\alpha$  is the time scale (s);  $\alpha$  is the ground thermal diffusivity (m<sup>2</sup>/s); and  $g$  is the so-called g-function (Eskilson, 1987). Due to lack of space, the approach used to compute the g-function of a BHE field will not be covered here but in a subsequent paper. Cimmino et al. (2013) provide a comprehensive review on the computation of g-functions.

### Borehole Equivalent Resistance

The second term of Equation 1 corresponds to the steady-state temperature variation between the heat carrier fluid and the borehole wall and depends on the equivalent borehole resistance  $R_b$ , which lumps together the fluid ( $R_f$ ), pipe ( $R_p$ ) and grout thermal resistances ( $R_g$ ) of the borehole.

The pipe thermal resistance is a function of the pipe thermal conductivity  $k_p$  (W/(mK)) and the inner and outer pipe radius  $r_i$  and  $r_o$  (m) as described by:

$$R_p = \frac{\ln r_o/r_i}{2\pi k_p} \quad (2)$$

The convective thermal resistance  $R_f$  is a function of fluid flow rate  $v$  (m<sup>3</sup>/s) and thermal properties. These parameters are either temperature dependent or affected by flow rate variations. A convenient way to express  $R_f$  is to connect it to the heat transfer coefficient  $h_i$  (W/(m<sup>2</sup>K)) through Equation 3.

$$R_f(v, T_f) = \frac{1}{2\pi r_i h_i(v, T_f)} \quad (3)$$

In Equation 3,  $h_i$  is a function of the fluid flow rate and mean fluid temperature. For given  $v$  and  $T_f$  values, the Reynolds, Prandtl and Nusselt numbers

are evaluated. Then, depending on the flow state,  $h_i$  is calculated using either the Hausen, Gnielinski and Dittus-Boelter correlations (Incropera et al., 2007).

To compute  $R_g$  the following expression, suggested by Hellström (1991) for 2-pipe BHE, is used:

$$R_g = \frac{1}{2\pi k_g} \left( \ln \frac{r_b}{r_o} + \ln \frac{r_b}{2D} + \frac{k_g - k_s}{k_g + k_s} \ln \frac{r_b^4}{r_b^4 - 1/D^4} \right) \quad (4)$$

where  $k_g$  is the grout thermal conductivity (W/(mK));  $k_s$  is the ground thermal conductivity (W/(mK));  $r_b$  is the borehole radius (m) and  $2D$  is the center-to-center pipe distance (m).

When an analytical approach, such as Equation 4, is used to evaluate  $R_g$ , the equivalent borehole resistance is given for a 2-pipe BHE by:

$$R_b(v, T_f) = 0.5(R_f(v, T_f) + R_p + R_g) \quad (5)$$

Alternatively, one may choose the multipole method (Bennet et al., 1987; Claesson and Hellström, 2011) to directly compute  $R_b$  based on a pair of  $R_f$  and  $R_p$  values. In this work,  $R_b(v, T_f)$  is precomputed for several fluid temperatures and flow rates and used for further multidimensional interpolations.

### Spatial and Temporal Superposition

In Equation 1, the last term corresponds to the mean borehole wall temperature change noted here as  $\Delta T_b$ . If the heat flux  $q$  varies with time, the temporal superposition principle is used to predict  $\Delta T_b(t)$ , provided the heat flux signal can be represented as a step function. For a time-varying step function,  $q(t)$ , the borehole wall temperature change,  $\Delta T_b$ , can be expressed as:

$$\Delta T_b(r_b, q, t) = \sum_{j=i}^{n_t} \frac{q(t_j) - q(t_{j-1})}{2\pi k} \cdot g\left(\frac{t - t_{j-1}}{t_s}, \frac{r_b}{H}\right) \quad (6)$$

where  $j$  is the time step index and  $n_t$  is the number of time steps before time  $t$ . Notice that at  $t_0 = 0$ ,  $q(t_0) = 0$ . For a given BHE field, Equation 6 reduces to:

$$\Delta T_b(r_b, q, t) = \sum_{j=i}^{n_t} f(t_j) \cdot g\left(\frac{t - t_{j-1}}{t_s}, \frac{r_b}{H}\right) \quad (7)$$

with  $f$ , the incremental heat flux function given by

$$f(t_j) = \frac{q(t_j) - q(t_{j-1})}{2\pi k} \quad (8)$$

As noted by Marcotte and Pasquier (2008), Equation 7 corresponds to the convolution product of functions  $f$  and  $g$ , noted  $(f * g)(t)$ . It is then possible to compute  $\Delta T_b$  with a spectral approach using discrete Fourier transforms ( $\mathcal{F}$ ) through:

$$\Delta T_b(t) = (f * g)(t) = \mathcal{F}^{-1}(\mathcal{F}(f) \cdot \mathcal{F}(g)) \quad (9)$$

Solving a convolution product, such as the one in Equation 9, using a spectral approach assumes that 1) a step function represents the heat flux signal, 2) all heat pulses are of equal duration and 3) the convolved functions are periodic. Since both  $f$  and  $g$  are aperiodic, the zero padding technique allows

modelling the correct temperatures. The latter consists to add  $2n_t - 1$  zeros at the end of vectors  $f$  and  $g$ , to solves Equation 9 with these zero-padded vectors, and to retain only the first  $n_t$  elements of the solution.

Many public domain software packages are available to compute a discrete Fourier transform and its inverse. For instance, the FFTW package (Frigo and Johnson, 2005) implements several Fast Fourier Transform (FFT) algorithms and it automatically selects the fastest algorithm for a given vector size and computer platform. It can be shown that solution of Equation 6 in the time domain for  $n_t$  time steps is of complexity  $O[n_t^2]$ . Since FFT algorithms are of complexity  $O[n_t \log(n_t)]$ , solving Equation 6 by a spectral approach is significantly faster.

### Integration of Heat Pumps

For a field of  $n_b$  boreholes having a total length  $L$  (m), the total ground load is equal to  $qL$ . If  $V$  is the volumetric flow rate ( $\text{m}^3/\text{s}$ ) circulating in each of the  $n$  operating HPs, the temperature difference  $\Delta T_{HP}$  (K) can be expressed by

$$\Delta T_{HP} = \frac{q \cdot L}{n \cdot V (\Delta T_{HP}) \cdot C_f (EWT)} \quad (10)$$

where  $C_f$  is the fluid volumetric heat capacity ( $\text{J}/(\text{K} \cdot \text{m}^3)$ ). Here,  $C_f$  is expressed as a function of the entering water temperature to capture the possible range of variation of  $C_f$  with temperature. To minimize pumping power, it can be advantageous to modulate the flow rate in the underground loop as a function either of  $EWT$ ,  $T_f$ ,  $n$  or  $\Delta T_{HP}$ . In Equation 10, the temperature difference  $\Delta T_{HP} = LWT - EWT$  across operating heat pumps is used to modulate the flow rate, which leads to a recursive relationship.

For a case where a first manifold distributes an equal flow rate of fluid  $V$  to each of the  $n_{HP}$  installed heat pumps, and where a second manifold distributes a flow rate of fluid  $v$  to each of the  $n_b$  BHEs, the total flow rate within the underground loop is given by  $n_{HP}V = n_b v$ . Therefore, assuming the heat carrier fluid is perfectly mixed before reaching the BHEs, the temperature difference between the fluid entering and leaving a BHE is given by

$$\Delta T_{BHE} = \Delta T_{HP} \frac{n}{n_{HP}} \quad (11)$$

Note if the heat pumps vary in size and design flow rates, equation 11 can be modified easily to capture such features.

The heat pumps entering water temperature on the source side ( $EWT$ ) relates to the mean fluid temperature through

$$T_f(t) = EWT + \frac{\Delta T_{BHE}}{2} \quad (12)$$

Combining equations 1, 5, 9 and 12 leads to

$$EWT(t) = T_g + q \cdot R_b + \Delta T_b - \frac{\Delta T_{BHE}}{2} \quad (13)$$

which expresses the entering water temperature on the heat pumps source side.

The coefficient of performance ( $COP$ ) and capacity ( $CAP$ ) (W/unit) of HPs depend on parameters such as fluid flow rate and temperatures on the source and load sides. For simplicity, the  $COP$  and  $CAP$  are expressed here as a function of fluid temperature on the source side only. The designation  $COP$  is used here to describe the HP performance for both heating and cooling modes (instead of using the EER for cooling). Therefore, the ground load  $q$  is given by:

$$q = \frac{Q_{HP}}{L} \left( 1 \pm \frac{1}{COP(EWT)} \right) \quad (14)$$

with  $Q_{HP}$  (W), the energy delivered by  $n$  operating HP units, given by

$$Q_{HP} = \pm n \cdot CAP(EWT) \quad (15)$$

In Equation 14 and 15, the  $\pm$  sign expresses the fact that for time steps corresponding to heating, the heating  $COP$  and  $CAP$  performance curves are used and their values are multiplied by -1. The sign convention used is such that  $Q_B$ ,  $Q_{HP}$  or  $q$  are negatives in heating mode. To account for HP not operated at full capacity, one should note that Equation 15 can be modified to integrate the heat pump part load factor (PLF).

In practice, several control strategies are used to modulate  $n$  and ensure that the  $EWT$  never exceeds the temperature limits of the heat pumps ( $EWT_H$  and  $EWT_C$ ) or that  $Q_{HP}$  doesn't exceed the total building load  $Q_B$ . In the proposed approach,  $n$  corresponds to the mean number of operating heat pumps over the time step duration. Therefore,  $n$  is a fractional number ranging from 0 to  $n_{HP}$ , the number of installed heat pumps.

### PROPOSED ALGORITHM

Combining equations 10 and 13 to 15 leads to a non-linear and recursive relationship requiring an iterative solution procedure. The solution process involves, at each of the  $n_t$  time steps, the interpolation of several dependent variables ( $COP$ ,  $CAP$ ,  $R_b$ ,  $v$ ) and identification, under constraints, of  $EWT$ ,  $n$  and  $q$  values. The problem can be seen as an inverse problem where  $n$  is the unknown time dependent signal to be found. To identify this signal, this work proposes the iterative algorithm presented in Fig. 2.

It should be stressed that solution of Equation 9 in the spectral domain provides, in a single step, values of  $\Delta T_b$  for each of the  $n_t$  time steps. Therefore, solution of Equation 10, 13, 14 and 15 (and interpolation of  $COP$ ,  $CAP$ ,  $R_b$  and  $v$ ) for each of the  $n_t$  time steps can be easily distributed over several processing units (CPU or GPU) to reduce computing time.

The following paragraphs describe the main computation steps and present some of the underlying features of the algorithm.

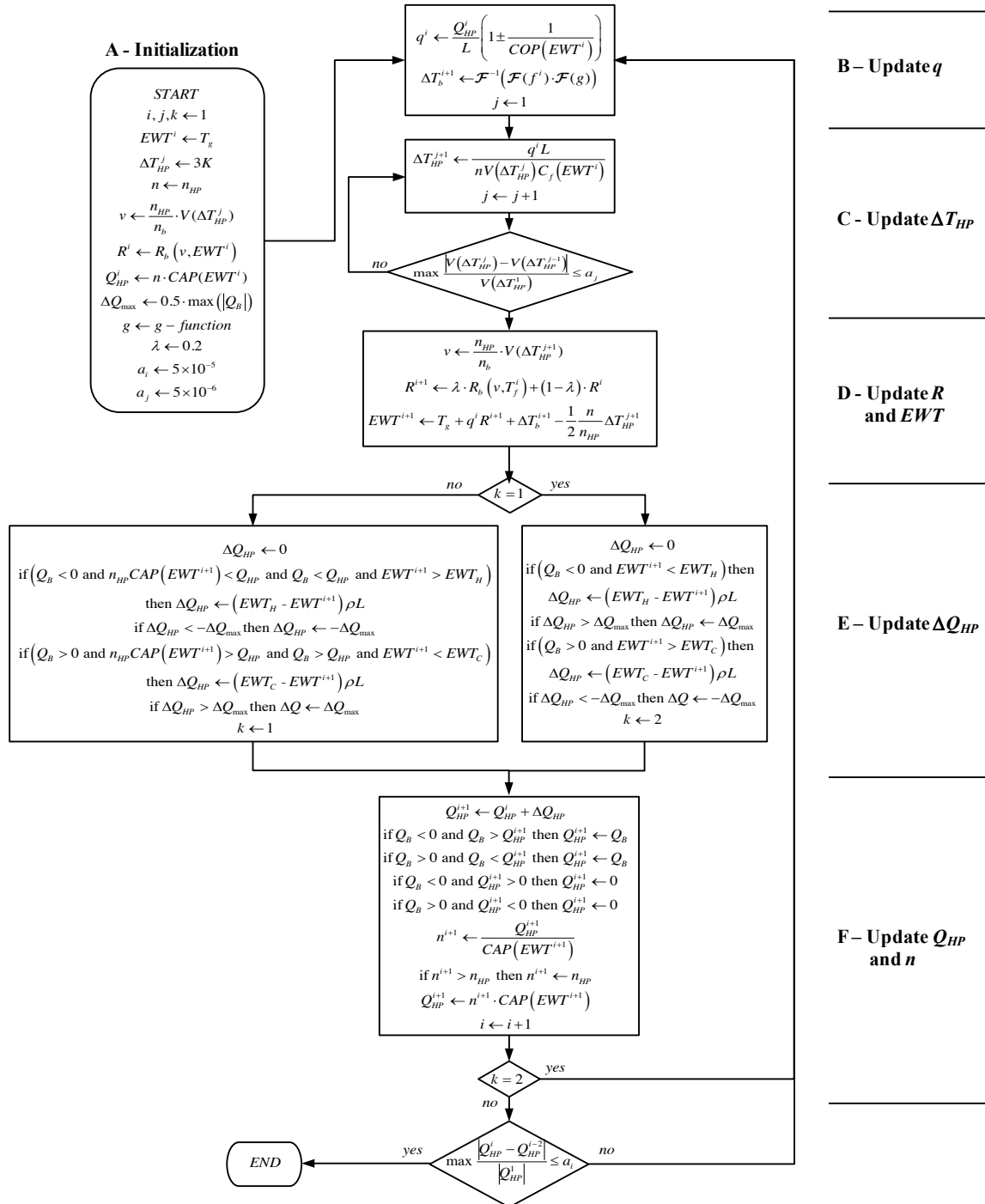


Figure 2: Proposed algorithm.

### A – Initialization of variables

Let  $i$  and  $j$  be the iteration counter for  $q$  and  $\Delta T_{HP}$  respectively. Also, let  $k$  be a switch with values of either 1 or 2. For the first outer iteration ( $i=1$ ), it is assumed that:  $EWT$  corresponds to the initial ground temperature  $T_g$ ; all heat pumps are initially in operation ( $n=n_{HP}$ ) and  $\Delta T_{HP}$  equals 3 °C.

### B – Update $q$

In step B, Equation 14 is used to update the ground loads  $q$  for time steps 1 to  $n_t$ . HP performance data are used to linearly interpolate the  $COP$  based on the  $EWT$  value at the current iteration.

As already mentioned, the performance curve corresponding to the heating or cooling mode is used to interpolate the  $COP$  for the time steps in heating or cooling mode respectively. During the iteration process,  $EWT$  can fall outside the range of  $COP$  data. In such situations, the nearest performance data is used and extrapolated (this also applies to the evaluation of  $CAP$ ,  $C_f$ ,  $v$  and  $R_b$ ).

With the updated  $q^i$  vector, Equations 8 and 9 are then used to compute the incremental heat flux function  $f$  and then  $\Delta T_b$ . For efficiency reasons,  $\Delta T_b$  is computed here in the spectral domain with vectors  $f$  and  $g$  padded with zeros but a similar result can be

obtained, albeit with a much larger computation time, if  $\Delta T_b$  was computed in the temporal domain with Equation 7.

### C – Update $\Delta T_{HP}$

The third step consists in evaluating  $\Delta T_{HP}$ , the temperature difference within one of the  $n$  operating HPs, by solving Equation 10. To ensure the reproduction of the flow rate modulation pattern (see Figure 4d for an example of modulation pattern), a recursive process is used and repeated until the maximum variation of  $V$  between two successive iterations (over all time steps) is smaller than the tolerance  $a_j$ .

### D – Update $R$ and $EWT$

In some cases, the flow in the pipes can vary from a laminar to a turbulent flow for small variations of  $v$  and  $T_f$ , which can induce a slow convergence rate. To dampen too large variations of  $R_b$  between two successive iterations, the updated  $R^{i+1}$  values are obtained by a linear combination of the resistances computed at the current and previous iteration with weights ( $\lambda$ ) and  $(1-\lambda)$  respectively. It was found that a value of  $\lambda$  of 0.2 provides stability, robustness and speed to the algorithm. The values computed previously allow to update the vector of entering water temperatures ( $EWT^{i+1}$ ).

### E – Update $\Delta Q_{HP}$

Step E evaluates  $\Delta Q_{HP}$ , the vector of corrections to  $Q_{HP}$ . These corrections are used in step F to update  $Q_{HP}$  with the following formula:

$$Q_{HP}^{i+1} = Q_{HP}^i + \Delta Q_{HP} \quad (16)$$

in a two-step process controlled by the switch variable  $k$ .

In the first step, if  $k=1$ , a correction  $\Delta Q_{HP}$  is computed to ensure that the entering water temperature does not exceed the heat pumps operational temperature limits. This correction is given by:

$$\Delta Q_{HP} = (EWT_{HPLim} - EWT^{i+1}) \rho L \quad (17)$$

and is chosen to be proportional to 1) the difference between  $EWT$  at the current iteration and the heat pump temperature limits and 2) a time dependent coefficient  $\rho$  (W/(mK)). In cooling mode (heating), if  $EWT^{i+1}$  is above (below) the heat pump temperature limit for a given time step, a negative (positive)  $\Delta Q_{HP}$  value is provided by Equation 17 which reduces (increases)  $Q_{HP}$  and  $EWT$  accordingly.

If  $k=2$ , a correction  $\Delta Q_{HP}$  is computed to account for situations where the  $EWT$  computed at the current iteration is within the HP temperature limits but where the building energy demand is greater than the energy provided by the HPs. In both cases ( $k=1$  or  $k=2$ ),  $\Delta Q_{HP}$  is limited to half the maximum building load to constrain the correction.

The strategy used here relies on a  $\rho$  function given by

$$\rho = \frac{q^*}{\Delta T_b^*} \quad (18)$$

where  $q^*$  (W/m) is a constant ground load and  $\Delta T_b^*$  is the corresponding borehole wall temperature variation computed by Equation 9. To ensure a sufficient convergence rate,  $\rho$  is constrained above a minimum threshold value of 1 W/(mK). This constraint ensures that  $\Delta Q_{HP}$  is at least equal to  $(EWT_{HPLim} - EWT^{i+1}) \cdot 1L$ .

At each iteration, a correction is brought to all components of  $q$  and a correction at a given time step will spread over the subsequent times. Since  $\rho$  is a regularly decreasing function, its role is to increase the correction for early time steps and to damp the correction for later time steps. The theoretical development supporting the computation of  $\rho$  is presented in a separate paper (Pasquier and Marcotte, 2013).

Table 1  
Parameters used in the numerical example.

PARAMETERS	VALUES
$r_b$	0.075 m
$2D$	0.090 m
$r_o$	0.021 m
$r_i$	0.017 m
$k_p$	0.40 W/(mK)
$k_g$	1.25 W/(mK)
$k_s$	3.00 W/(mK)
$C_s$	2.2 MJ/(m <sup>3</sup> ·K)
$T_g$	10 °C
$n_{HP}$	10 HP
$EWT_H$	-2 °C
$EWT_C$	35 °C
$a_i$	$5 \times 10^{-5}$ -
$a_j$	$5 \times 10^{-5}$ -

### F – Update $Q_{HP}$ and $n$

In step F,  $Q_{HP}$  is updated with Equation 16 and constraints are applied to the updated values to ensure that  $Q_{HP}$  does not exceed the building thermal load  $Q_B$ .

To find the number of operating HPs at each time step, Equation 19 is used and constrained to ensure that  $n^{i+1}$  does not exceed the number of installed HP.

$$n^{i+1} = \frac{Q_{HP}^{i+1}}{CAP(EWT^{i+1})} \quad (19)$$

Finally, an updated vector  $Q_{HP}$  is again computed with Equation 19 before proceeding to the next outer iteration. The iterative process stops when the maximum variation of  $Q_{HP}$  between successive iterations is smaller than the tolerance  $a_i$ .

## EXAMPLE

To illustrate the versatility and flexibility of the algorithm presented in this work, an example is

presented in this section. The studied borehole field layout is presented in Figure 3 and is composed of a mix of 20 boreholes of varying dip and strike angles, and whose lengths vary from 20 to 50 m.

The input parameters used in this example are summarized in Table 1 while the input  $COP$  and  $CAP$  curves as well as the modulation patterns for  $V$  are shown in Figure 6. This example uses a synthetic building load profile as shown in Figures 4a and 5a. The simulation is performed every hour for a 10-year period ( $n_t=87\ 600$  time steps).

## RESULTS AND DISCUSSION

Figure 4 presents the temporal evolution of the building load ( $Q_B$ ), the total heat pumps capacity ( $Q_{HP}$ ), the entering water temperature ( $EWT$ ), the number of operating heat pump ( $n$ ) and the flow rate ( $V$ ) for a 10-year period while Figure 5 presents a close-up view for the first 8 760 hours of operation.

It can be seen that the fluid temperature reaches the temperature limits of the heat pumps specified in Table 1. In order not to exceed these limits, the algorithm has reduced the number of operating heat pumps ( $n$ ) accordingly. Therefore, for some time steps, the heat pump capacity is smaller than the building load (even if an excess capacity is available). In such situations, an auxiliary heating or cooling system fills in the remaining energy needs. Recall that  $n$  (and therefore  $Q_{HP}$ ) corresponds to the mean number of operating heat pump over the time step duration. Even if an oscillating pattern is clearly visible on Fig. 5c), this pattern is caused by the building energy demand perceptible on Fig. 5a), not by HP on-off cycles.

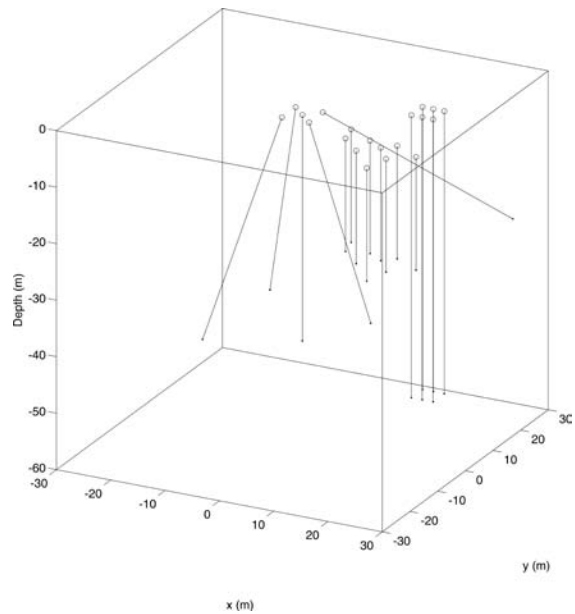


Figure 3: Layout of the borehole field used in the numerical example.

As time progresses, the number of operating HPs shown in Fig 4c) increases during heating periods. This is a consequence of a progressive increase of the  $EWT$  at the beginning of each winter, which allows using a greater portion of the installed capacity. Notice that the ninth installed HP works only 1.06% of the operating time while the last one is never used, indicating a non-optimal design of the system.

Fig. 6a) compares the input flow rate patterns (solid red or blue lines) and the flow rates obtained at the last iteration (small black dots). Two small clusters of data are visible for  $\Delta T_{HP}$  near  $-1.5^\circ\text{C}$  and  $3^\circ\text{C}$ . These data points correspond to situations where  $EWT$  is around the HP temperature limits. For such situations, the algorithm increases the flow rate to

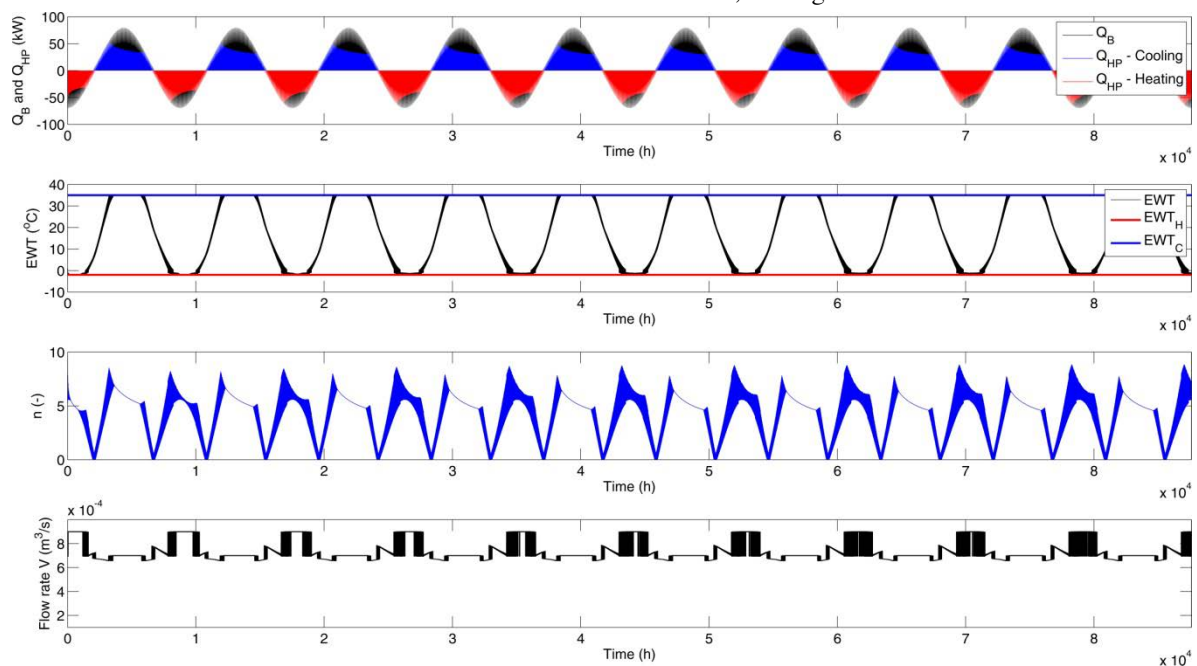


Figure 4: Evolution of a) building and heat pump loads, b) entering water temperature, c) number of operating heat pump and d) flow rate in each heat pump for a 10-year period.

maintain, if possible, a fully developed turbulent flow and increase heat transfer. Since the flow rate patterns of Fig. 6a) are different for heating and cooling modes, the maximum flow rates shown on Fig. 4d) and 5d) are also different.

The equivalent borehole thermal resistances obtained at the last iteration (see Fig 6b) are regrouped in two lines. The top line presents higher resistances and corresponds to the cooling mode. These slightly higher  $R_b(v, T_f)$  values are a consequence of the lower maximum flow rate specified for cooling mode. Note that for time steps in laminar flow (low  $T_f$  values),  $R_b$  is significantly higher. A cluster of low  $R_f$  values is visible for fluid temperature around  $-2^\circ\text{C}$ . These data correspond to situations where the flow rate within the BHEs is constrained to the maximum prescribed value in order to minimize the convective resistance.

Figures 6c) and d) compare the input  $COP$  and  $CAP$  curves (solid red or blue lines) to the values used by the algorithm at the last iteration (small black dots). The figures show that, as designed, the  $COP$  and  $CAP$  values are correctly interpolated between the performance data while for  $EWT$  outside the available data, the last value is extrapolated.

The simulation presented here was carried out on a desktop computer with an Intel® Core i7 980 CPU under Matlab® 2012a. Convergence was reached in 76 iterations and in only 9.9 seconds (without the computation of the g-function). The problem presented here is numerically demanding. For conventional real-world problems, a solution is usually obtained in less than 8 seconds.

## CONCLUSION

This paper presented an efficient method to simulate a hybrid ground-coupled heat pump system, which results in a fast evaluation of the energy supplied by the heat pumps and the auxiliary subsystems (boiler or cooling tower) on an hourly basis.

In the proposed approach, the response function of a BHE field is convolved in the spectral domain with a ground load signal to predict the variation of the ground temperature. The equivalent borehole thermal resistance is expressed as a function of the heat carrier fluid temperatures and flow rates to accommodate variations of the convective resistance.

At each time step, the algorithm evaluates the ground load based on the building heating or cooling energy demand, and the coefficient of performance and capacity of the heat pumps, which are expressed as a function of the fluid temperature. To capture the nonlinearity between the fluid temperature and the ground load, an iterative process is used. The approach used solves the entire simulation duration in a single step.

Several constraints are added to regulate the energy provided by each subsystem, to ensure that the fluid temperature remains always between the heat pumps operational temperature limits and that the total energy provided to the building never exceeds the capacity of the heat pumps.

## ACKNOWLEDGEMENT

This research was financed by a Natural Sciences and Engineering Research Council of Canada (NSERC) research grant.

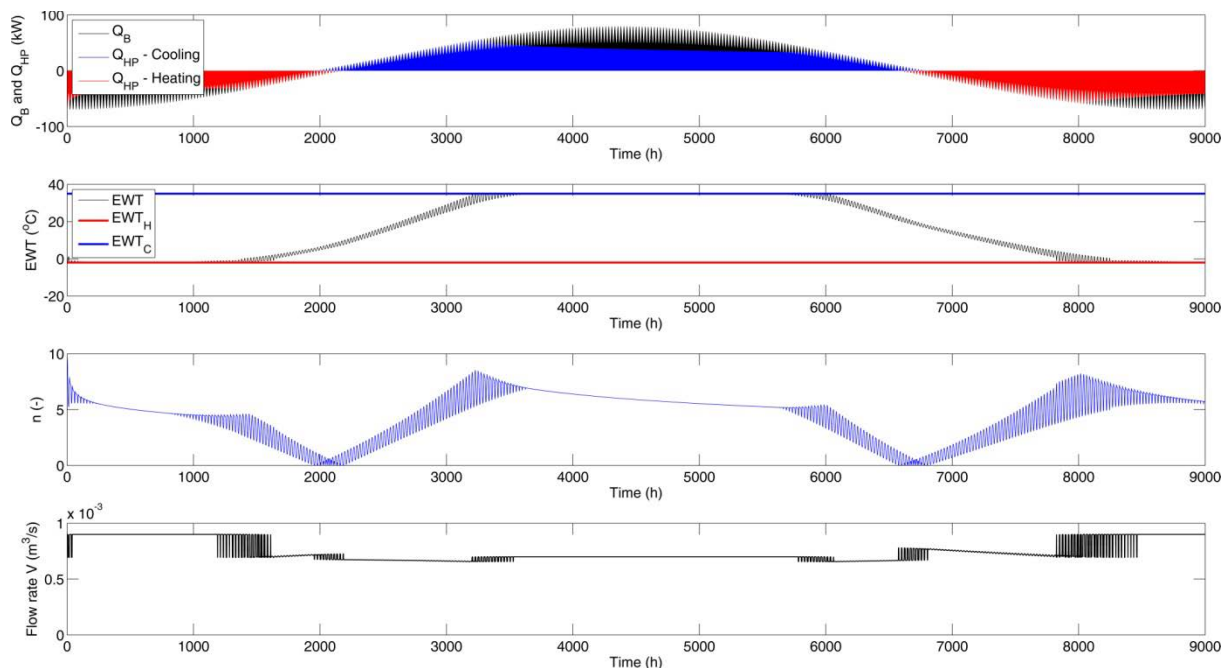


Figure 5: Evolution of a) building and heat pump loads, b) entering water temperature, c) number of operating heat pump and d) flow rate in each heat pump for the first 8760 hours.



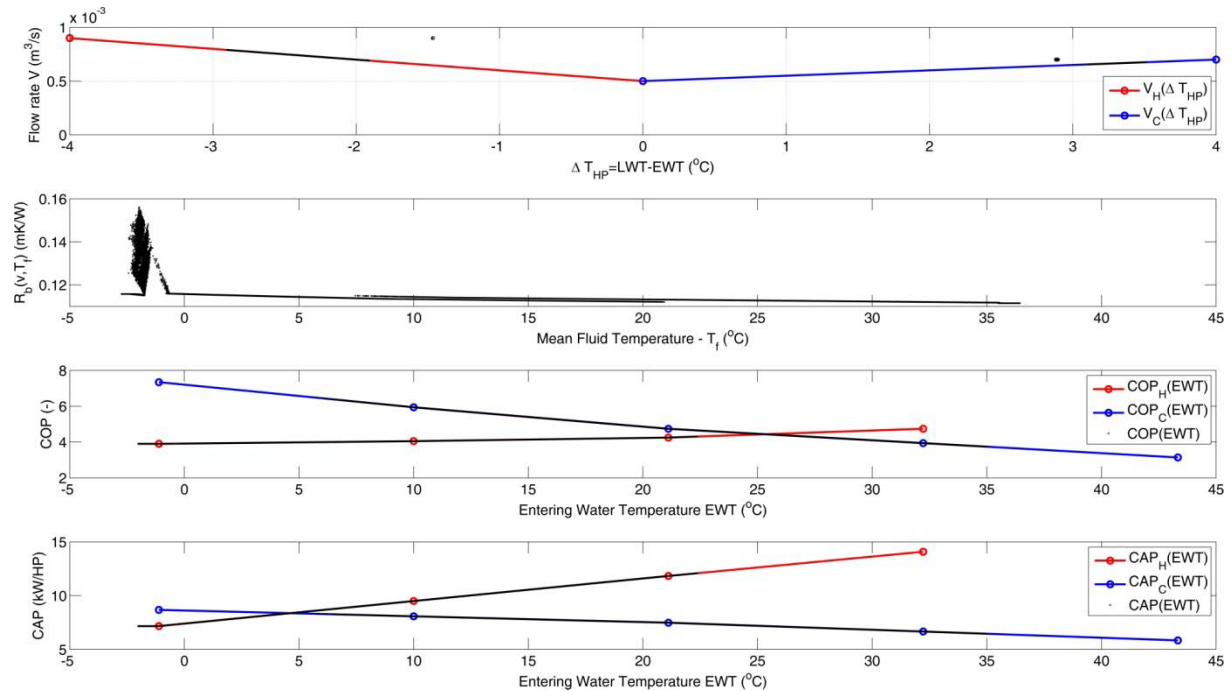


Figure 6: Input and computed values for a) flow rate modulation pattern  $V$ , b)  $R_b$ , c) COP, and d) CAP.

## REFERENCES

- Bennet, J., Claesson, J. and Hellström, G., 1987. *Multipole Method to Compute the Conductive Heat Flows to and between Pipes in a Composite Cylinder*, Lund, Sweden: University of Lund, Department of Building Technology and Mathematical Physics.
- Cimmino, M., Bernier, M. and Adams, F., 2013. A contribution towards the determination of g-functions using the finite line source. *Applied Thermal Engineering*, 51(1-2), pp.401–412.
- Claesson, J. and Hellström, G., 2011. Multipole method to calculate borehole thermal resistances in a borehole heat exchanger. *HVAC&R Research*, 17(6), pp.895–911.
- Cullin, J.R. and Spitler, J.D., 2011. A Computationally Efficient Hybrid Time Step Methodology for Simulation of Ground Heat Exchangers. *Geothermics*, 40(2), pp.144–156.
- Eskilson, P., 1987. *Thermal Analysis of heat extraction borehole*. Lund, Sweden: University of Lund.
- Frigo, M. and Johnson, S.G., 2005. The Design and Implementation of FFTW3. *Proceedings of the IEEE*, 93(2), pp.216–231.
- Gentry, J.E., J.D. Spitler, D.E. Fisher, and X. Xu. 2006. Simulation of Hybrid Ground Source Heat Pump Systems and Experimental Validation. In *The 7th International Conference on System Simulation in Buildings*. Liège, Belgium.
- Hellström, G. (1991). *Ground Heat Storage - Thermal Analysis of Duct Storage Systems - Theory*. Doctoral Thesis, University of Lund, Sweden.
- Incropera, F.P., DeWitt, D.P., Bergman, T.L. and A.S. Lavine, *Fundamentals of Heat and Mass Transfer*, Sixth Edition, John Wiley and Sons, New York, 2007.
- Marcotte, D. and Pasquier, P. 2008. Fast Fluid and Ground Temperature Computation for Geothermal Ground-Loop Heat Exchanger Systems. *Geothermics*, 37(6), pp.651–665.
- Marcotte, D. and Pasquier, P. 2009. The Effect of Borehole Inclination on Fluid and Ground Temperature for GLHE Systems. *Geothermics*, 38(4), pp.392–398.
- Nagano, K., Katsura, T. and Takeda, S., 2006. Development of a design and performance prediction tool for the ground source heat pump system. *Applied Thermal Engineering*, 26(14-15), pp.1578–1592.
- Pahud D. and Hellström G. (1996) The New Duct Ground Heat Model for TRNSYS. In *Proceedings of Eurotherm, Physical Models for Thermal Energy Stores*, 25-27 March, pp. 127 – 136. Eindhoven, The Netherlands,
- Pasquier, P. and Marcotte, D., 2013. Efficient Computation of Heat Flux Signals Ensuring Reproduction of Prescribed Temperatures at Several Interacting Heat Sources. Submitted to *Applied Thermal Engineering*.